Inorganic Nitrate Promotes the Browning of White Adipose Tissue through the Nitrate-Nitrite-Nitric Oxide Pathway

Lee D Roberts[1,2,*], **Tom Ashmore**[2,3], **Aleksandra O Kotwica**[3], **Steven A Murfitt**[2], **Bernadette O Fernandez**[4], **Martin Feelisch**[4], **Andrew J Murray**[#3], and **Julian L Griffin**[1,2,*]

[1]Medical Research Council – Human Nutrition Research, Elsie Widdowson Laboratory, 120 Fulbourn Road, Cambridge, CB2 9NL, UK

[2]Department of Biochemistry and Cambridge Systems Biology Centre, University of Cambridge, 80 Tennis Court Road, Old Addenbrooke's Site, Cambridge, CB2 1GA, UK

[3]Department of Physiology, Development and Neuroscience, University of Cambridge, Downing Street, Cambridge, CB2 3EG, UK

[4]Faculty of Medicine, Clinical & Experimental Sciences, University of Southampton, Southampton General Hospital, Tremona Road, Southampton, SO16 6YD, UK

[#] These authors contributed equally to this work.

Abstract

Inorganic nitrate was once considered an oxidation end-product of nitric oxide metabolism with little biological activity. However, recent studies have demonstrated that dietary nitrate can modulate mitochondrial function in man and is effective in reversing features of the metabolic syndrome in mice. Using a combined histological, metabolomics, and transcriptional and protein analysis approach we mechanistically define that nitrate not only increases the expression of thermogenic genes in brown-adipose tissue but also induces the expression of brown adipocyte-specific genes and proteins in white adipose tissue, substantially increasing oxygen consumption and fatty acid β-oxidation in adipocytes. Nitrate induces these phenotypic changes through a mechanism distinct from known physiological small molecule activators of browning, the recently identified nitrate-nitrite-nitric oxide pathway. The nitrate-induced browning effect was enhanced in hypoxia, a serious co-morbidity affecting white adipose tissue in obese individuals, and corrected impaired brown adipocyte-specific gene expression in white adipose tissue in a murine model of obesity. Since resulting beige/brite cells exhibit anti-obesity and anti-diabetic effects, nitrate may be an effective means of inducing the browning response in adipose tissue to treat the metabolic syndrome.

Keywords

Nitrate; White Adipose Tissue; Thermogenesis; Hypoxia; Nitrite; Metabolomics

[*]**Corresponding Authors:** Lee D. Roberts. MRC Human Nutrition Research, Elsie Widdowson Laboratory, 120 Fulbourn Road, Cambridge, UK. CB1 9NL. Lee.Roberts@mrc-hnr.cam.ac.uk Tel.: +44 1223 427678 or Julian L. Griffin. MRC Human Nutrition Research, Elsie Widdowson Laboratory, 120 Fulbourn Road, Cambridge, UK. CB1 9NL. Jules.Griffin@mrc-hnr.cam.ac.uk Tel.: + 44 1223 764922.

The diffuse and complex nature of the metabolic syndrome integrates peripheral insulin resistance and visceral obesity with cardiovascular disease; making the discovery of underlying molecular mechanisms that unite the aspects of the metabolic syndrome both challenging and essential. The perturbation of nitric oxide (NO) synthesis and signaling has emerged as a potential modulator of both cardiovascular morbidity and metabolic dysfunction (1; 2).

Until recently inorganic nitrate was considered a non-bioactive product of NO oxidation (3). However, a number of studies have identified nitrate treatment of humans and rodents as having effects similar to NO (4; 5). The discovery of anti-obesity effects of nitrate in rodents, including weight loss, a reduction of body fat, reversal of lipodystrophy and an improvement in glucose and insulin homeostasis, may highlight nitrate as having therapeutic potential for the treatment of the metabolic syndrome (6).

Dietary nitrate increases the circulating concentration of cGMP in humans (7) and low nitrate/nitrite diets decrease steady-state concentrations of cGMP in a number of tissues (8). Recently, cGMP has been shown to regulate energy balance in white adipocytes (9). The development of a brown adipocyte-like phenotype in white adipocytes, a process known as "browning", includes the induction of thermogenesis, the dissipation of chemical energy to produce heat (10; 11). Peroxisome proliferator activated receptor γ co-activator 1α (PGC-1α) activates key components of the thermogenic program in white adipocytes, including fatty acid oxidation, mitochondrial biogenesis, and increased oxygen consumption (12). The thermogenic process occurs through the activity and increased expression of several brown-adipocyte specific genes including uncoupling protein 1 (UCP1), an inner mitochondrial membrane protein that uncouples the mitochondrial proton gradient (13). Cells expressing brown-adipocyte specific genes are interspersed within the white adipose tissue (WAT) of rodents and humans (so-called "beige" or "brite" cells) (14; 15)) and demonstrate anti-diabetic and anti-obesity effects in rodent models (16-19). The recent discovery of a physiological small molecule activator of browning in WAT highlights metabolites as both potential mediators of the thermogenic response and therapeutics for the metabolic syndrome (20).

In this study we investigate the effect of nitrate on WAT metabolism both in the classic experimental model of browning *in vitro,* the mouse primary adipocyte, and *in vivo* in mice and rats to establish whether this may, in part, explain the anti-obesity activity of nitrate. We demonstrate that nitrate increases the expression of brown-adipocyte specific genes and concordant proteins within white adipocytes to confer a brown-adipocyte like phenotype.

Research Design and Methods

Animal Experimentation

Male Wistar rats (6 weeks old) (269 ± 2 g; n = 24) (Charles River.) were weight matched and received either distilled water or water containing sodium nitrate (NaNO$_3$) (0.35, 0.7, 1.4 mM; n = 6/group) (Ultra-pure, Sigma-Aldrich) ad libitum for 18 days with food and water intake monitored. Animals were housed in conventional cages at room temperature with a 12-hour/12-hour light/dark photoperiod. In the hypoxia study, male Wistar rats (6

weeks old) were weight matched and separated into two groups (n = 10/group), housed in either normoxic or normobaric hypoxic environments (hypoxia chamber: 13% O_2, with 20 air changes per hour). The rats in each group received either distilled water containing NaCl (n = 5, 0.7mM NaCl) or water containing $NaNO_3$ (0.7 mM; n = 5) for 14 days. All other details are as above.

Male p129 mice (6 weeks old) received either distilled water containing NaCl (0.7mM, Control, n = 7) or $NaNO_3$ (0.7mM, n = 7) (Ultra-pure, Sigma-Aldrich) ad libitum for 15 days with food and water intake monitored.

ob/ob mice (n = 10) and C57bl/6 wild type mice (n = 10) (9 weeks old, The Jackson Laboratory) received either distilled water containing NaCl (0.7mM, Control, n = 5) or $NaNO_3$ (0.7mM, n = 5) (Ultra-pure, Sigma-Aldrich) ad libitum for 8 weeks with food and water intake monitored. Animals were housed in conventional cages at room temperature with a 12-hour/12-hour light/dark photoperiod.

All animals had micro-nutrient levels normalized by a standardized quality controlled (SQC) diet (RM1 (E); 55% crude carbohydrate, 3% crude fat, 15% crude protein; Special Diets Services, UK) one week prior to study commencement. The nitrate content of this diet is 2 mg/Kg and the nitrite content was undetectable below a threshold of 1 mg/Kg.

All procedures were carried out in accordance with UK Home Office protocols by a personal license holder.

Blood and Tissue Collection

Rats and mice were euthanized with sodium pentobarbital (200 mg/ml, Vétoquinol UK Ltd.). Blood was obtained by cardiac puncture, collected in N-ethylmaleimide/EDTA (10 and 2.5 mM, respectively) containing tubes and immediately centrifuged to obtain plasma. WAT and interscapular brown adipose tissue (iBAT) were removed and flash frozen in liquid nitrogen.

Histology

WAT was fixed for 24 hr in 10% formalin and washed for 1 hr in PBS before being set in wax. The tissue was then cut into 8 μm thick slices and stained with haematoxylin and eosin.

Plasma Nitrate Measurements

Plasma nitrate was measured as described previously (21).

Culture and Differentiation of Primary Adipocytes

Primary white adipose stromal vascular cells were fractionated from 6 – 10 week old C57BL6 male mice as previously described (22). Stromal vascular cells were then cultured and differentiated into adipocytes according to published methods (22; 23). During the 6 day differentiation, cells were cultured with either saline (control), 25 μM $NaNO_3$, 50 μM $NaNO_3$ or 500 μM $NaNO_3$ (Ultra-pure, Sigma-Aldrich) or, during the investigation of the effects of sodium nitrite ($NaNO_2$), with saline (control), 50 μM $NaNO_2$ or 500 μM $NaNO_2$

(Ultra-pure, Sigma-Aldrich). The pharmacological inhibitor studies utilized 2-Phenyl-4,4,5,5-tetramethylimidazoline-1-oxyl 3-oxide (PTIO) (50 μM), NG-nitro-L-arginine methyl ester (L-NAME) (1 mM), 1H-[1,2, 4]oxadiazolo[4,3-a]quinoxalin-1-one (ODQ) (1 μM) (Sigma-Aldrich) and KT5823 (1 μM) (Santa Cruz Biotechnology). Cells were treated with PTIO, L-NAME, ODQ or KT5823 with and without 500 μM $NaNO_3$. $NaNO_3$ and inhibitors were added at day 1 of differentiation. In the hypoxia study, cells were isolated and differentiated as above. Hypoxic conditions were achieved using a New Brunswick Eppendorf Galaxy 14S incubator supplied with nitrogen and set to maintain a 2% O_2 environment.

siRNA Xanthine Oxidoreductase Knockdown

FlexiTube siRNA against XOR, AllStars negative control siRNA and HiPerFect Transfection Reagent were purchased from Qiagen. Transfection of primary adipocytes was carried out as per the manufacturer's instructions (75 ng siRNA, 3 μl transfection reagent per well,10 nM final siRNA concentration) on day 2 and 4 of differentiation.

Tissue and Primary Adipocyte Metabolite Extraction

Metabolites were extracted from WAT and primary adipocytes as previously described (24).

^{13}C-palmitate Substrate Labeling Study

Palmitate was solubilized using a dialyzed albumin solution (24). At 6 days post-differentiation medium was removed from primary adipocytes and replaced with serum free media containing insulin 850 nM, triiodothyronin 1 nM, and rosiglitazone 1 μM and 140 μM U-^{13}C labeled palmitate (Cambridge Isotope Laboratories). After 2 days cells were collected and metabolites extracted as previously described. During the 8 days of the experiments duration, cells were cultured with either saline (control), 50 μM $NaNO_3$ or 500 μM $NaNO_3$.

Gene Expression Analysis

Total RNA extraction from WAT, BAT, and adipocytes, cDNA conversion and quantitative RT-PCR was performed according to published protocols (20). All data were normalized to 18SrRNA (mouse WAT, BAT and adipocytes) or RLPL1 (rat WAT) and quantitative measures obtained using the - -CT method.

Protein Analysis

Analysis of UCP1 and PGC-1α was performed using ELISA as per the manufacturer's instructions (UCP1 Kit SEF557Ra, PGC-1α Kit SEH337Ra, Cloud-Clone Corp. Houston, TX, USA). Immunoblotting for CPT1 was carried out as previously described (25).

Citrate Synthase Assay

Citrate synthase was assayed according to Houle-Leroy et al.(26).

White Adipocyte Respirometry

Oxygen consumption rates were measured in white adipocytes (250,000 cells) maintained in Krebs-Henseleit buffer at 37°C, using Clark-type oxygen electrodes (Strathkelvin Instruments, Strathkelvin, UK) as described previously (27).

Gas Chromatography-Mass Spectrometry Analysis

Dried aqueous and organic phase samples were derivatized using the method described previously (24). Gas Chromatography-Mass Spectrometry (GC-MS) and data analysis were performed according to published methods (24).

^{13}C-labeled Substrate GC-MS Analysis

Analysis of organic and aqueous phases was carried out as described above and according to published methods (24).

Liquid Chromatography-Mass Spectrometry Analysis of Intact Lipids

Liquid Chromatography-Mass Spectrometry (LC-MS) was performed on WAT using a Waters Q-ToF Xevo mass spectrometer (Waters Corporation, Manchester, UK) operating with electrospray ionization in combination with an Acquity UPLC according to the method described by Roberts at al. (24). LC-MS spectra and chromatograms were analyzed using the MarkerLynx Application MassLynx (version 4.1; Waters Corporation) using published protocols (24).

LC-MS Analysis of cGMP

LC-MS analysis of cGMP was performed using a 4000 QTRAP triple quadrupole mass spectrometer (Applied Biosystems/Sciex), coupled to an Acquity UPLC (Waters Corporation, Manchester, UK) according to a previously described method (28). The multiple reaction monitoring parameters for cGMP were: Q1 = 346.13 m/z, Q3 = 152.1 m/z, collision energy = 23, declustering potential = 41, collision cell exit potential = 10.

Statistical Analyses

Error bars represent standard error of the mean. P-values were calculated by either one-way or two-way ANOVA as stated with a Dunnett's *post-hoc* test when multiple comparisons where made solely to control and a Tukey's *post-hoc* test when comparisons were made between all treatment groups.

Results

Nitrate Induces a Brown Adipocyte-like Phenotype in White Adipocytes In Vivo

Rodents treated with dietary nitrate are protected against diabetes and obesity (6). Activation of the browning response in WAT may represent a process underlying this altered systemic energy balance; therefore, we assessed the effect of dietary nitrate on the expression of brown adipocyte-specific genes in WAT *in vivo*. Wistar rats were treated with 0.35 mM, 0.7 mM or 1.4 mM NaNO$_3$ in drinking water for 18 days based on preliminary dose escalation studies. Plasma nitrate concentrations were found to increase in a dose-dependent fashion,

with the basal concentration in control rats at 11.1 ± 0.7 μM, increasing to 15.4 ± 2.0 μM, 22.8 ± 4.0 μM, and 32.6 ± 5.0 μM in the rats treated with 0.35 mM, 0.7 mM and 1.4 mM $NaNO_3$, respectively. Water and food intake was not significantly different between the groups (Table S1). Since it is the subcutaneous WAT that has the greatest predisposition to undergo browning and influence energy balance (23), we concentrated our analyses on the inguinal WAT depot. Nitrate dose-dependently increased brown adipocyte-specific gene expression in WAT. The expression of UCP-1 was increased, as was the molecular marker of brown-like adipocytes, cell death-inducing DFFA-like effector a (CIDEA), which has a role in the regulation of the thermogenic process (Fig. 1*A*). Expression of PGC-1α, and the mitochondrial electron transport chain component cytochrome *c* (CYCS) were increased dose-dependently. Nitrate also increased expression of β-oxidation genes including carnitine palmitoyltransferase 1 (CPT1) and acyl-CoA dehydrogenase, very long chain (ACADvl) (Control vs. 0.35 mM $NaNO_3$ P 0.01, Control vs. 0.7 mM $NaNO_3$ P 0.0001, Control vs. 1.4 mM $NaNO_3$ P 0.001). Specific beige-selective genes, including T-box transcription factor (Tbx1), Transmembrane Protein 26 (Tmem26) and CD137, distinguish beige fat cells from both classical brown and white adipocytes (29). Nitrate moderately increased the expression of the beige-selective markers Tbx1, Tmem26 and CD 137 specifically characterizing these cells as beige adipocytes within the inguinal WAT depot (Fig. S1). Nitrate did not significantly change the expression of the canonical adipocyte-specific markers adiponectin (ADIPOQ) and fatty acid binding protein 4 (FABP4) in the WAT indicating that adipose tissue exposed to nitrate presents similar levels of adipogenesis (Fig. S2). Furthermore, analysis of brown-adipocyte specific gene expression in the visceral (epididymal) WAT of nitrate treated rats also revealed a moderate increase in the mRNA of several genes involved in the thermogenic and browning process (Fig. S3).

To determine whether changes in the expression of key brown adipocyte-specific genes were translated to the level of protein, the concentrations of UCP-1, PGC-1α and CPT1 protein in the subcutaneous WAT of nitrate treated rats were analyzed. Nitrate increased the expression of the brown-adipocyte specific proteins UCP-1 and PGC-1α (Control vs. 0.35 mM $NaNO_3$ P 0.001, Control vs. 0.7 mM $NaNO_3$ P 0.05, Control vs. 1.4 mM $NaNO_3$ P = 0.01) (Fig 1.*B*). Nitrate also increased the concentration of the β-oxidation protein CPT1 within WAT (Control vs. 0.35 mM $NaNO_3$ P 0.05, Control vs. 0.7 mM $NaNO_3$ P 0.05, Control vs. 1.4 mM $NaNO_3$ P 0.05) (Fig. 1 *C*). The observed induction of characteristic brown adipocyte genes and increase in the concentration of brown adipocyte-specific proteins suggests a browning of the subcutaneous WAT.

We next examined whether the changes in gene and protein expression induced by nitrate resulted in altered energy metabolism within the WAT. The activity of citrate synthase, a marker of mitochondrial density and TCA cycle flux, was significantly increased following nitrate treatment, suggesting increased mitochondrial biogenesis consistent with browning of WAT (Control vs. 0.35 mM $NaNO_3$ P 0.05, Control vs. 0.7 mM $NaNO_3$ P 0.05, Control vs. 1.4 mM P 0.01) (Fig. 1 *D*). Since beige/brite cells utilize fatty acids as fuel for thermogenesis, we investigated whether nitrate affected lipid metabolism in the WAT of treated rats. GC-MS and LC-MS were utilized to measure total fatty acid and triacylglycerol (TAG) species in the WAT, respectively. Nitrate treatment increased the medium chain fatty

acid (MCFA) (laurate, myristate) / long chain fatty acid (LCFA) (arachidate, behenate) ratio, indicative of increased β-oxidation shortening fatty acid chain length (Control vs. 0.35 mM $NaNO_3$ P 0.05, Control vs. 0.7 mM $NaNO_3$ P 0.05, Control vs. 1.4 mM $NaNO_3$ P 0.01) (Fig. 1*E* and Fig. S4). LC-MS analysis demonstrated that nitrate also decreased the total TAG content within WAT (0.95-fold, 0.35 mM $NaNO_3$; 0.94-fold, 0.7 mM $NaNO_3$; 0.98-fold, 1.4 mM $NaNO_3$; Control vs. 0.35 mM P 0.01, Control vs. 0.7 mM P 0.01) (Fig. 1*F*). Therefore, metabolic changes induced in WAT *in vivo* by nitrate treatment were characteristic of a brown adipocyte-like phenotype.

Histological analyses of the inguinal WAT of nitrate treated rats at fifty-times magnification revealed the presence of fascicles of multilocular brown adipocyte-like cells (Fig 1*G*). Under greater magnification the smaller multilocular brown adipocyte-like cells can be observed confirming morphological changes in the WAT. Together these data indicate that nitrate induces the browning of WAT.

To ensure nitrate-induced expression of brown adipocyte-specific genes in rat WAT is not species-specific, mice were treated with 0.7 mM $NaNO_3$ in drinking water. As in rat, brown adipocyte-specific gene expression was increased in inguinal WAT by nitrate treatment (Fig. S5A). The expression of thermogenic genes in classical iBAT from nitrate treated mice was also increased (Fig. S5B).

Nitrate Induces a Brown Adipocyte-like Phenotype in White Adipocytes In Vitro

Nitrate may function directly to increase the expression of brown adipocyte-specific genes in WAT or indirectly through metabolic bioactivation in cells distinct from those in the target tissue. Therefore stromal vascular fraction-derived primary adipocytes isolated from inguinal WAT of mice were treated with nitrate. $NaNO_3$ concentrations of 25 μM, 50 μM and 500 μM were chosen. The latter two concentrations correspond to plasma levels in mice exhibiting improved metabolic phenotypes when chronically treated and acutely dosed with 0.1 mmol/kg of $NaNO_3$, respectively (6). Nitrate treatment significantly increased the expression of brown-adipocyte specific genes UCP-1, CIDEA and PGC-1α. Also increased in expression were CYCS, CPT1 and ACADvl (Control vs. 25 μM $NaNO_3$ P 0.01, Control vs. 50 μM $NaNO_3$ P 0.0001, Control vs. 500 μM $NaNO_3$ P 0.0001) (Fig. 2 *A*). By contrast, nitrate did not significantly affect the expression of a panel of classical mature adipocyte-specific genes including ADIPOQ, FABP4, and adipsin, suggesting that nitrate dose not directly affect adipogenesis per se (Fig. S6) (29). These data indicate nitrate mediated induction of brown-adipocyte specific gene expression occurs directly at the WAT.

We next investigated whether the transcriptional changes induced by nitrate conferred functional effects on energy expenditure in primary adipocytes. The O_2 consumption rates of adipocytes treated with nitrate (50 μM and 500 μM) were measured (Fig. 2*B*). The basal O_2 consumption rate was dose-dependently increased in adipocytes treated with nitrate (Control 3.1 nmoles O_2/min/10^6 cells, 50 μM $NaNO_3$ 4.5 nmoles O_2/min/10^6 cells, 500 μM $NaNO_3$ 5.1 nmoles O_2/min/10^6 cells, P 0.05). Maximal respiratory rates were probed using excess succinate (20 mM) (27), and were found to increase in adipocytes treated with nitrate (Control 4.2 nmoles O_2/min/10^6 cells, 50 μM $NaNO_3$ 6.6 nmoles O_2/min/10^6 cells, 500 μM

$NaNO_3$ 7.7 nmoles O_2/min/10^6 cells, P 0.05). These findings indicate that nitrate increases the respiration of adipocytes consistent with the browning response (Control vs. 50 μM $NaNO_3$ P 0.01, Control vs. 500 μM $NaNO_3$ P 0.001).

GC-MS analysis of the fatty acid metabolism of adipocytes treated with nitrate also highlighted the increase in the MCFA/LCFA ratio, mirroring the effects observed in WAT *in vivo* (Control vs. 50 μM $NaNO_3$ P 0.05, Control vs. 500 μM $NaNO_3$ P = 0.08) (Fig. 2*C*).

Nitrate Increases Fatty Acid Uptake and β-oxidation in White Adipocytes In Vitro

To confirm the increased β-oxidation observed in nitrate treated adipocytes, the stable isotope substrate U-^{13}C-palmitate was used to monitor flux through the fatty acid oxidation pathway. Primary adipocytes were incubated in serum-free media containing U-^{13}C-palmitate and treated with nitrate. GC-MS analysis was used to determine the relative enrichment of metabolites. Nitrate significantly increased the ^{13}C enrichment of palmitate (C16:0) in adipocytes, indicating increased fatty acid uptake (P 0.01) (Fig. 3 *A*). Enrichment of shorter chain fatty acids, myristate (C14:0) and laurate (C12:0) was also increased in nitrate treated adipocytes (C14:0 P 0.05, C12:0 P 0.05) (Fig. 3 *B* and 3*C*), consistent with augmented chain shortening through β-oxidation.

The labeled fatty acids are catabolized releasing labeled acetyl-CoA which enters the TCA cycle. Nitrate treatment increased the labeling of TCA cycle intermediates, citrate (Control vs. 50 μM $NaNO_3$ P 0.0001, Control vs. 500 μM $NaNO_3$ P 0.001) (Fig. 3 *D*), succinate (Control vs. 500 μM $NaNO_3$ P 0.05) (Fig. 3 *E*) and malate (Control vs. 500 μM $NaNO_3$ P 0.05) (Fig. 3*F*). Therefore, nitrate confers a functional effect on white adipocytes, increasing flux through fatty acid β-oxidation. Taken together, these data demonstrate that nitrate induces the expression of thermogenic genes and the development of a brown-fat like phenotype in white adipocytes and WAT.

Nitrate Functions through the Nitrate-Nitrite-NO Pathway to Induce Browning of Adipocytes

In addition to the classical L-arginine-nitric oxide synthase (NOS)-NO pathway, NO can also be generated *in vivo* from nitrate through serial reduction to nitrite and then to NO via the nitrate-nitrite-NO pathway (30). Therefore, we hypothesized that nitrate might be functioning via NO to produce the browning response in WAT. Primary adipocytes were differentiated in the presence of nitrate and the NO scavenger PTIO (Fig. 4*A*) (Control vs. 500 μM $NaNO_3$ P 0.0001, 500 μM $NaNO_3$ vs. 500 μM $NaNO_3$ + 50 μM PTIO P 0.0001). Sequestration of NO by PTIO negated the nitrate-induced expression of brown adipocyte-specific genes, indicating that nitrate indeed functions via NO to induce browning.

To exclude the induction of NO production through the L-arginine-NOS-NO pathway as a mechanism of nitrate stimulated browning, control experiments were conducted using the non-isoform selective NOS inhibitor L-NAME. Inhibition of NOS did not affect nitrate-stimulated brown adipocyte-specific gene expression in adipocytes (Fig. 4*B*) (Control vs. 500 μM $NaNO_3$ P 0.001, Control vs. 500 μM $NaNO_3$ + 1mM L-NAME P 0.0001, 500

μM NaNO$_3$ vs. 500 μM NaNO$_3$ + 1mM L-NAME not significant). Therefore, nitrate stimulated browning functions through NO but independently of NOS.

An enzymatic mechanism for the reduction of nitrate to NO in mammals, catalyzed by XOR, was recently reported (4). XOR is expressed in WAT and has a role in adipocyte homeostasis (31). Nitrate dose-dependently increased the expression of XOR in primary adipocytes (Fig. 4*C*). Using PTIO, the nitrate stimulated increase in XOR expression was demonstrated to be mediated through NO (Fig. 4*D*). The expression of XOR in primary adipocytes was knocked down by approximately 80% using siRNA (Fig 4*E*). Knockdown of XOR abrogated the nitrate-induced expression of brown adipocyte-specific genes in white adipocytes (Fig 4*F*). Consistent with these results, nitrite promoted brown adipocyte-specific gene expression in adipocytes via an NO-dependent mechanism (Fig. S7*A, B*). By examining fold-increases of brown adipocyte-specific genes, nitrite at equivalent concentrations to nitrate appeared more potent in inducing the browning response, consistent with the inefficient overall rate of reduction of nitrate to nitrite and eventually NO (4). These results indicate that nitrate mediated browning of adipocytes requires XOR and the reduction of nitrate to NO.

Nitrate Increases Browning of Adipocytes Through a cGMP and Protein Kinase G Mediated Mechanism

We next characterized the downstream signaling/effector pathways mediating nitrate-induced browning of WAT. NO activates cGMP signaling through stimulation of soluble guanylyl cyclase (3). cGMP mediates browning of WAT (9) suggesting cGMP signaling as a potential mechanism underlying nitrate-induced browning. Therefore, we measured the concentration of cGMP in nitrate treated adipocytes using LC-MS (Fig. 5*A*). Nitrate increased the concentration of cGMP in adipocytes, from 2.7 pmoles/10^6 cells in the control to 5.2 pmoles/10^6 cells and 4.9 pmoles/10^6 cells in the 50 μM NaNO$_3$ and 500 μM NaNO$_3$ treated cells, respectively (P = 0.04, Control vs. 50 μM NaNO$_3$ P 0.05, Control vs. 500 μM NaNO$_3$ P 0.05) (Fig. 5 *B*). Similarly, analysis of WAT from rats demonstrates an increase in cGMP concentrations *in vivo*, following nitrate treatment (P < 0.05, Control vs. 0.35mM NaNO$_3$ P 0.01, Control vs. 0.7mM NaNO$_3$ P 0.05, Control vs. 1.4mM NaNO$_3$ P = 0.07) (Fig. 5*C*).

The pharmacological inhibitor of guanylyl cyclase, ODQ, was used to confirm a cGMP-dependent mechanism for nitrate-induced browning. Inhibition of guanylyl cyclase abolished the nitrate-induced expression of brown adipocyte-specific genes in white adipocytes (Control vs. 500 μM NaNO3 P 0.0001, 500 μM NaNO3 vs. 500 μM NaNO3 + 1 μM ODQ P 0.001) (Fig. 5 *D*).

The cGMP-dependent protein kinase G (PKG) is expressed in the WAT of rodents and is a key regulator of adipocyte function (9; 32). Using a pharmacological inhibitor of PKG (KT5823) we investigated the role of this protein kinase in the nitrate-induced browning response. Inhibition of PKG abrogated the nitrate-induced expression of brown-adipocyte specific genes in the adipocytes (Control vs. 500 μM NaNO3 P 0.0001, 500 μM NaNO3 vs. 500 μM NaNO3 + 1 μM KT5823 P 0.0001) (Fig. 5 *E*). Therefore, the mechanism

underlying nitrate-induced browning of WAT functions through the cGMP/PKG signaling axis.

Nitrate Induced Browning of WAT is Enhanced In Hypoxia

Unlike the L-arginine-NOS-NO pathway, which is dependent on oxygen, production of NO through the nitrate-nitrite-NO pathway is augmented as oxygen concentrations decrease (33) and may regulate tissue adaptations to hypoxia (34; 35). Since the nitrate-induced browning of WAT is mediated through the nitrate-nitrite NO pathway, we examined the capacity of nitrate to increase brown adipocyte-specific gene expression in adipocytes during hypoxia.

Primary adipocytes were treated with $NaNO_3$ (50 μM) in low oxygen conditions (2% O_2). These oxygen concentrations correspond to levels observed in obese WAT (36). In parallel, adipocytes from the same stromal vascular isolation were treated with $NaNO_3$ (50 μM) under normoxic conditions. Since nitrate-induced browning requires the reduction of nitrate to NO, and XOR functions to reduce nitrate to NO (4), we assessed the expression of XOR in the adipocytes in response to changes in oxygen availability. XOR expression was found to increase in adipocytes exposed to hypoxia, an effect enhanced by simultaneous nitrate treatment (Fig. 6*A*) (Normoxia Control vs. Hypoxia Control P 0.01, Hypoxia Control vs. Hypoxia 50 μM $NaNO_3$ P 0.05, Normoxia 50 μM $NaNO_3$ vs. Hypoxia 50 μM $NaNO_3$ P 0.001). Nitrate also increased the expression of brown adipocyte-specific genes in both the normoxia and hypoxia conditioned cells (Normoxia Control vs. Normoxia 50 μM $NaNO_3$ P 0.0001, Hypoxia Control vs. Hypoxia 50 μM $NaNO_3$ P 0.0001) (Fig. S8 *A*). Hypoxia *per se* significantly decreased the expression of the brown-adipocyte specific genes compared to normoxia (Normoxia Control vs. Hypoxia Control P 0.01). However, nitrate increased the expression of the brown-adipocyte specific genes and fully restored the expression of UCP1, CIDEA and CPT1 under hypoxia to levels greater than that of normoxic controls. The decrease in expression of the genes due to hypoxia alone was corrected for by normalizing the hypoxia conditioned cells to hypoxia control to facilitate comparison of the fold-changes in expression of the browning genes following nitrate treatment (Fig. 6*B*). The fold-change increase of brown adipocyte-specific gene expression in hypoxic adipocytes treated with nitrate compared to hypoxic control was significantly greater than that observed in normoxic cells (Normoxia 50 μM $NaNO_3$ vs. Hypoxia 50 μM $NaNO_3$ P 0.0001).

To investigate the enhanced browning effect of nitrate in WAT under hypoxic conditions *in vivo*, rats were housed in a hypoxia chamber and either received 0.7mM NaCl or 0.7 mM $NaNO_3$ in their drinking water for 14 days. A parallel group of rats were identically treated but housed in a normoxic environment. Water and food intake was not significantly different between the groups (Table S2). As *in vitro*, XOR expression was increased in WAT of rats exposed to hypoxia, and further enhanced by nitrate treatment (Fig. 6*C*) (Normoxia Control vs. Hypoxia Control P 0.01, Normoxia 50 μM $NaNO_3$ vs. Hypoxia 50 μM $NaNO_3$ P 0.01). As expected, nitrate increased expression of brown adipose-specific genes in WAT during normoxia (Normoxia Control vs. Normoxia 0.7 mM $NaNO_3$, P 0.01) (Fig. 6 *D*). Brown adipocyte-specific gene expression was also increased in the WAT of rats treated with nitrate under hypoxic conditions (Hypoxia Control vs. Hypoxia 0.7 mM $NaNO_3$, P < 0.0001). Interestingly, brown adipocyte-specific gene expression within WAT was

significantly increased in the rats treated with nitrate during hypoxia when compared to those treated with nitrate and housed in a normoxic environment (Normoxia 0.7 mM $NaNO_3$ vs. Hypoxia 0.7mM $NaNO_3$, P < 0.0001). The expression of ADIPOQ was not significantly affected by either nitrate or hypoxia (Fig. S8*B*). Overall, these data indicate that the nitrate-induced expression of brown adipocyte-specific genes in WAT is augmented in hypoxia.

The WAT of obese humans and rodents is in a hypoxic state that perturbs metabolism, increasing glycolysis and de novo lipogenesis and decreasing fatty acid breakdown, further contributing to the pathology of obesity (36-39). Therefore, we investigated the effect of dietary nitrate on the expression of brown adipocyte-specific genes in WAT in a rodent model of obesity, the *ob/ob* mouse. Wild-type C57bl/6 and *ob/ob* mice received either 0.7 mM NaCl or 0.7 mM $NaNO_3$ in their drinking water for 8 weeks. Plasma nitrate concentrations were elevated from 59.8 μM ± 4 and 53.8 μM ± 11 in the chloride treated C57bl/6 and *ob/ob* mice respectively to 373.1 ± 73 and 323.9 ± 58 in their nitrate treated counterparts. The expression of several brown adipocyte-specific genes in the WAT of *ob/ob* mice was significantly reduced when compared to wild-type mice. Nitrate increased the expression of the brown adipocyte-specific genes, partially restoring the impaired levels of expression in this model of obesity (Fig 6*E*).

Discussion

Nitrate was considered a non-bioactive metabolite of NO and a potentially toxic dietary constituent. However, studies showing that nitrate reduces blood pressure (5; 7; 40) and the oxygen demand of exercise (41) indicated that this anion may be beneficial for metabolic health. Complementary studies demonstrated that nitrate has anti-obesity and anti-diabetic effects, independent of increased mitochondrial biogenesis or PGC1α expression in liver or muscle, in endothelial NOS-deficient mice, a strain prone to a metabolic syndrome-like phenotype (6). Similar anti-diabetic effects of nitrate have since been described in Sprague-Dawley rats (42). Diets low in nitrate and nitrite reduce the concentration of cGMP in certain tissues (8). In recent years a role for cGMP signaling in systemic energy balance has emerged (32; 43; 44). cGMP was recently demonstrated to induce browning within WAT (9). These beige/brite cells (14; 15) have cardiometabolic protective effects in rodents (11; 16; 18; 19; 22; 23; 45). Thus, we hypothesized that nitrate might contribute to the improved metabolic phenotype by inducing the browning response in WAT.

In the present study we demonstrate that nitrate increases the expression of thermogenic genes in BAT and activates a brown adipocyte-like transcriptional and functional phenotype within WAT. Furthermore, we find that nitrate induces browning of adipocytes through the NOS-independent nitrate-nitrite-NO pathway. Thus nitrate activates the thermogenic process in a manner distinct from physiological metabolite activators of browning previously described (Fig. S9) (20). Our findings suggest a mechanism by which nitrate is reduced to NO, which in turn increases cGMP production via soluble guanylyl cyclase activation. Increased cGMP concentrations activate PKG, increasing the expression of PGC-1α and other key browning genes such as UCP1 and CIDEA in white adipocytes. Increased expression of brown adipocyte-specific and β-oxidation pathway genes translates to a brown adipocyte-like functional phenotype characterized by increased fatty acid β-oxidation (Fig.

7). Incidentally, the recently identified mechanism for natriuretic peptide induced browning of WAT was also revealed to signal through the cGMP cascade (43), underscoring the importance of this signaling pathway for the physiological activation of thermogenesis in WAT.

It was observed that the nitrate-induced browning response in WAT was enhanced in hypoxia. The nitrate-nitrite-NO pathway is significantly augmented during hypoxia, with both the activity and expression of XOR increased in low oxygen conditions (4). The pathway has also been implicated in the adaptive response of some tissues to hypoxia (30; 33; 35). It is conceivable that production of NO from nitrate leads to the enhanced nitrate-induced browning of WAT observed in hypoxia. The WAT of obese humans, and genetic and dietary models of obesity in rodents, is in a hypoxic state (36; 37). Exposure of adipocytes to hypoxia leads to cellular metabolic reprogramming, consisting of increased glycolysis and fatty acid and TAG synthesis and decreased fatty acid catabolism, that contributes to the pathology of obesity (38; 39). The identification of an enhanced capacity for nitrate to induce the browning response of WAT in low oxygen conditions through NO, which will likely also contribute to improved vascular health in obese individuals where NO production is decreased (46), may represent a significant therapeutic opportunity to partly reverse this hypoxia mediated pathological state. Indeed, our studies show that the impaired expression of several brown adipocyte-specific genes in the WAT of the *ob/ob* mouse model of obesity is partially reversed by nitrate treatment.

From a nutritional perspective, humans are exposed to nitrate as part of their daily diet, with green leafy vegetables representing a significant source of the anion. A high vegetable component to diets is consistently shown to have a protective role in the development of metabolic morbidity (47; 48). It has been suggested that the high nitrate content of vegetables is partly responsible for their association with cardiometabolic protection (30; 34). It is worth speculating that increasing the flux through the nitrate-nitrite-NO pathway may be one mechanism through which dietary vegetable consumption confers the associated metabolic protection. Given that the concentrations of nitrate utilized in our study are readily achievable through dietary vegetable consumption (6; 34), dietary nitrate may also function to activate cGMP signaling in human WAT. The possibility that this ubiquitous dietary constituent could induce browning of WAT in humans is tantalizing.

It should be noted that the responses of WAT to nitrate were not universally dose-dependent. This observation may represent rapid tachyphylaxis and/or resistance to inorganic nitrate, a phenomenon well characterized in the clinical use of organic nitrates, in particular at high doses. Alternatively, cellular uptake of inorganic nitrate may become rate-limiting or saturated at high doses. The NO signaling pathway is also subject to counter regulation through a number of disparate mechanisms that include the action of phosphodiesterases (PDEs), which may influence the effect of nitrate in WAT (Fig S10). PDEs such as PDE5, control cGMP concentrations and therefore inhibit downstream effects such as protein kinase G stimulation. Indeed, inhibition of PDE5 is known to stimulate the browning of WAT (9).

In summary, we identify nitrate as a novel non-β-adrenergic activator of the browning response in WAT and highlight this small anion as both a potential dietary mediator of protection from, and potential therapeutic modality for the treatment of, metabolic disease.

Supplementary Material

Refer to Web version on PubMed Central for supplementary material.

Acknowledgments

References

1. Huang PL. eNOS, metabolic syndrome and cardiovascular disease. Trends Endocrinol Metab. 2009; 20:295–302. [PubMed: 19647446]

2. Monti LD, Barlassina C, Citterio L, Galluccio E, Berzuini C, Setola E, Valsecchi G, Lucotti P, Pozza G, Bernardinelli L, Casari G, Piatti P. Endothelial nitric oxide synthase polymorphisms are associated with type 2 diabetes and the insulin resistance syndrome. Diabetes. 2003; 52:1270–1275. [PubMed: 12716763]

3. Moncada S, Higgs A. The L-arginine-nitric oxide pathway. N Engl J Med. 1993; 329:2002–2012. [PubMed: 7504210]

4. Jansson EA, Huang L, Malkey R, Govoni M, Nihlen C, Olsson A, Stensdotter M, Petersson J, Holm L, Weitzberg E, Lundberg JO. A mammalian functional nitrate reductase that regulates nitrite and nitric oxide homeostasis. Nat Chem Biol. 2008; 4:411–417. [PubMed: 18516050]

5. Larsen FJ, Ekblom B, Sahlin K, Lundberg JO, Weitzberg E. Effects of dietary nitrate on blood pressure in healthy volunteers. N Engl J Med. 2006; 355:2792–2793. [PubMed: 17192551]

6. Carlstrom M, Larsen FJ, Nystrom T, Hezel M, Borniquel S, Weitzberg E, Lundberg JO. Dietary inorganic nitrate reverses features of metabolic syndrome in endothelial nitric oxide synthase-deficient mice. Proc Natl Acad Sci U S A. 2010; 107:17716–17720. [PubMed: 20876122]

7. Kapil V, Milsom AB, Okorie M, Maleki-Toyserkani S, Akram F, Rehman F, Arghandawi S, Pearl V, Benjamin N, Loukogeorgakis S, Macallister R, Hobbs AJ, Webb AJ, Ahluwalia A. Inorganic nitrate supplementation lowers blood pressure in humans: role for nitrite-derived NO. Hypertension. 2010; 56:274–281. [PubMed: 20585108]

8. Bryan NS, Fernandez BO, Bauer SM, Garcia-Saura MF, Milsom AB, Rassaf T, Maloney RE, Bharti A, Rodriguez J, Feelisch M. Nitrite is a signaling molecule and regulator of gene expression in mammalian tissues. Nat Chem Biol. 2005; 1:290–297. [PubMed: 16408059]

9. Mitschke MM, Hoffmann LS, Gnad T, Scholz D, Kruithoff K, Mayer P, Haas B, Sassmann A, Pfeifer A, Kilic A. Increased cGMP promotes healthy expansion and browning of white adipose tissue. FASEB J. 2013; 27:1621–1630. [PubMed: 23303211]

10. Cannon B, Nedergaard J. Brown adipose tissue: function and physiological significance. Physiol Rev. 2004; 84:277–359. [PubMed: 14715917]

11. Lowell BB, Spiegelman BM. Towards a molecular understanding of adaptive thermogenesis. Nature. 2000; 404:652–660. [PubMed: 10766252]

12. Wu Z, Puigserver P, Andersson U, Zhang C, Adelmant G, Mootha V, Troy A, Cinti S, Lowell B, Scarpulla RC, Spiegelman BM. Mechanisms controlling mitochondrial biogenesis and respiration through the thermogenic coactivator PGC-1. Cell. 1999; 98:115–124. [PubMed: 10412986]

13. Enerback S, Jacobsson A, Simpson EM, Guerra C, Yamashita H, Harper ME, Kozak LP. Mice lacking mitochondrial uncoupling protein are cold-sensitive but not obese. Nature. 1997; 387:90–94. [PubMed: 9139827]

14. Ishibashi J, Seale P. Beige Can Be Slimming. Science. 2010; 328:1113–1114. [PubMed: 20448151]

15. Petrovic N, Walden TB, Shabalina IG, Timmons JA, Cannon B, Nedergaard J. Chronic Peroxisome Proliferator-activated Receptor gamma (PPAR gamma) Activation of Epididymally Derived White Adipocyte Cultures Reveals a Population of Thermogenically Competent, UCP1-containing Adipocytes Molecularly Distinct from Classic Brown Adipocytes. Journal of Biological Chemistry. 2010; 285:7153–7164. [PubMed: 20028987]

16. Cousin B, Cinti S, Morroni M, Raimbault S, Ricquier D, Penicaud L, Casteilla L. Occurrence of Brown Adipocytes in Rat White Adipose-Tissue - Molecular and Morphological Characterization. J Cell Sci. 1992; 103:931–942. [PubMed: 1362571]

17. Oberkofler H, Dallinger G, Liu YM, Hell E, Krempler F, Patsch W. Uncoupling protein gene: quantification of expression levels in adipose tissues of obese and non-obese humans. J Lipid Res. 1997; 38:2125–2133. [PubMed: 9374134]

18. Melnyk A, Harper ME, HimmsHagen J. Raising at thermoneutrality prevents obesity and hyperphagia in BAT-ablated transgenic mice. Am J Physiol-Reg I. 1997; 272:R1088–R1093.

19. Kopecky J, Clarke G, Enerback S, Spiegelman B, Kozak LP. Expression of the mitochondrial uncoupling protein gene from the aP2 gene promoter prevents genetic obesity. J Clin Invest. 1995; 96:2914–2923. [PubMed: 8675663]

20. Roberts LD, Bostrom P, O' Sullivan JF, Schinzel RT, Lewis GD, Dejam A, Lee YK, Palma MJ, Calhoun S, Georgiadi A, Chen MH, Ramachandran VS, Larson MG, Bouchard C, Rankinen T, Souza AL, Clish CB, Wang TJ, Estall JL, Soukas AA, Cowan CA, Spiegelman BM, Gerszten RE. beta-Aminoisobutyric Acid Induces Browning of White Fat and Hepatic beta-Oxidation and Is Inversely Correlated with Cardiometabolic Risk Factors. Cell Metab. 2014; 19:96–108. [PubMed: 24411942]

21. Rassaf T, Bryan NS, Kelm M, Feelisch M. Concomitant presence of N-nitroso and S-nitroso proteins in human plasma. Free Radic Biol Med. 2002; 33:1590–1596. [PubMed: 12446216]

22. Bostrom P, Wu J, Jedrychowski MP, Korde A, Ye L, Lo JC, Rasbach KA, Bostrom EA, Choi JH, Long JZ, Kajimura S, Zingaretti MC, Vind BF, Tu H, Cinti S, Hojlund K, Gygi SP, Spiegelman BM. A PGC1-alpha-dependent myokine that drives brown-fat-like development of white fat and thermogenesis. Nature. 2012; 481:463–U472. [PubMed: 22237023]

23. Seale P, Conroe HM, Estall J, Kajimura S, Frontini A, Ishibashi J, Cohen P, Cinti S, Spiegelman BM. Prdm16 determines the thermogenic program of subcutaneous white adipose tissue in mice. J Clin Invest. 2011; 121:96–105. [PubMed: 21123942]

24. Roberts LD, Murray AJ, Menassa D, Ashmore T, Nicholls AW, Griffin JL. The contrasting roles of PPARdelta and PPARgamma in regulating the metabolic switch between oxidation and storage of fats in white adipose tissue. Genome Biol. 2011; 12:R75. [PubMed: 21843327]

25. Morash AJ, Kotwica AO, Murray AJ. Tissue-specific changes in fatty acid oxidation in hypoxic heart and skeletal muscle. Am J Physiol Regul Integr Comp Physiol. 2013; 305:R534–541. [PubMed: 23785078]

26. Houle-Leroy P, Garland T Jr. Swallow JG, Guderley H. Effects of voluntary activity and genetic selection on muscle metabolic capacities in house mice Mus domesticus. J Appl Physiol (1985). 2000; 89:1608–1616. [PubMed: 11007602]

27. Charalambous M, Ferron SR, da Rocha ST, Murray AJ, Rowland T, Ito M, Schuster-Gossler K, Hernandez A, Ferguson-Smith AC. Imprinted Gene Dosage Is Critical for the Transition to Independent Life. Cell Metabolism. 2012; 15:209–221. [PubMed: 22326222]

28. Roberts LD, Souza AL, Gerszten RE, Clish CB. Targeted metabolomics. Curr Protoc Mol Biol. 2012 Chapter 30:Unit 30 32 31-24.

29. Wu J, Bostrom P, Sparks LM, Ye L, Choi JH, Giang AH, Khandekar M, Virtanen KA, Nuutila P, Schaart G, Huang K, Tu H, van Marken Lichtenbelt WD, Hoeks J, Enerback S, Schrauwen P, Spiegelman BM. Beige adipocytes are a distinct type of thermogenic fat cell in mouse and human. Cell. 2012; 150:366–376. [PubMed: 22796012]

30. Lundberg JO, Gladwin MT, Ahluwalia A, Benjamin N, Bryan NS, Butler A, Cabrales P, Fago A, Feelisch M, Ford PC, Freeman BA, Frenneaux M, Friedman J, Kelm M, Kevil CG, Kim-Shapiro DB, Kozlov AV, Lancaster JR Jr. Lefer DJ, McColl K, McCurry K, Patel RP, Petersson J, Rassaf T, Reutov VP, Richter-Addo GB, Schechter A, Shiva S, Tsuchiya K, van Faassen EE, Webb AJ, Zuckerbraun BS, Zweier JL, Weitzberg E. Nitrate and nitrite in biology, nutrition and therapeutics. Nat Chem Biol. 2009; 5:865–869. [PubMed: 19915529]

31. Cheung KJ, Tzameli I, Pissios P, Rovira I, Gavrilova O, Ohtsubo T, Chen Z, Finkel T, Flier JS, Friedman JM. Xanthine oxidoreductase is a regulator of adipogenesis and PPAR gamma activity. Cell Metabolism. 2007; 5:115–128. [PubMed: 17276354]

32. Haas B, Mayer P, Jennissen K, Scholz D, Berriel Diaz M, Bloch W, Herzig S, Fassler R, Pfeifer A. Protein kinase G controls brown fat cell differentiation and mitochondrial biogenesis. Sci Signal. 2009; 2:ra78. [PubMed: 19952371]

33. Castello PR, David PS, McClure T, Crook Z, Poyton RO. Mitochondrial cytochrome oxidase produces nitric oxide under hypoxic conditions: implications for oxygen sensing and hypoxic signaling in eukaryotes. Cell Metab. 2006; 3:277–287. [PubMed: 16581005]

34. Lundberg JO, Weitzberg E, Gladwin MT. The nitrate-nitrite-nitric oxide pathway in physiology and therapeutics. Nat Rev Drug Discov. 2008; 7:156–167. [PubMed: 18167491]

35. van Faassen EE, Bahrami S, Feelisch M, Hogg N, Kelm M, Kim-Shapiro DB, Kozlov AV, Li H, Lundberg JO, Mason R, Nohl H, Rassaf T, Samouilov A, Slama-Schwok A, Shiva S, Vanin AF, Weitzberg E, Zweier J, Gladwin MT. Nitrite as regulator of hypoxic signaling in mammalian physiology. Med Res Rev. 2009; 29:683–741. [PubMed: 19219851]

36. Ye JP, Gao ZG, Yin J, He Q. Hypoxia is a potential risk factor for chronic inflammation and adiponectin reduction in adipose tissue of ob/ob and dietary obese mice. Am J Physiol-Endoc M. 2007; 293:E1118–E1128.

37. Hosogai N, Fukuhara A, Oshima K, Miyata Y, Tanaka S, Segawa K, Furukawa S, Tochino Y, Komuro R, Matsuda M, Shimomura I. Adipose tissue hypoxia in obesity and its impact on adipocytokine dysregulation. Diabetes. 2007; 56:901–911. [PubMed: 17395738]

38. Krishnan J, Danzer C, Simka T, Ukropec J, Walter KM, Kumpf S, Mirtschink P, Ukropcova B, Gasperikova D, Pedrazzini T, Krek W. Dietary obesity-associated Hif1 alpha activation in adipocytes restricts fatty acid oxidation and energy expenditure via suppression of the Sirt2-NAD(+) system. Gene Dev. 2012; 26:259–270. [PubMed: 22302938]

39. Wellen KE, Thompson CB. Cellular Metabolic Stress: Considering How Cells Respond to Nutrient Excess. Mol Cell. 2010; 40:323–332. [PubMed: 20965425]

40. Webb AJ, Patel N, Loukogeorgakis S, Okorie M, Aboud Z, Misra S, Rashid R, Miall P, Deanfield J, Benjamin N, MacAllister R, Hobbs AJ, Ahluwalia A. Acute blood pressure lowering, vasoprotective, and antiplatelet properties of dietary nitrate via bioconversion to nitrite. Hypertension. 2008; 51:784–790. [PubMed: 18250365]

41. Larsen FJ, Schiffer TA, Borniquel S, Sahlin K, Ekblom B, Lundberg JO, Weitzberg E. Dietary inorganic nitrate improves mitochondrial efficiency in humans. Cell Metab. 2011; 13:149–159. [PubMed: 21284982]

42. Essawy S, Khaled AS, Amani E. Comparing the Effects of Inorganic Nitrate and Allopurinol in Renovascular Complications of Metabolic Syndrome in Rats: Role of Nitric Oxide and Uric Acid. Acta Endocrinol-Buch. 2012; 8:387–401.

43. Bordicchia M, Liu DX, Amri EZ, Ailhaud G, Dessi-Fulgheri P, Zhang CY, Takahashi N, Sarzani R, Collins S. Cardiac natriuretic peptides act via p38 MAPK to induce the brown fat thermogenic program in mouse and human adipocytes (vol 122, pg 1022, 2012). Journal of Clinical Investigation. 2012; 122:1584–1584.

44. Nisoli E, Clementi E, Paolucci C, Cozzi V, Tonello C, Sciorati C, Bracale R, Valerio A, Francolini M, Moncada S, Carruba MO. Mitochondrial biogenesis in mammals: the role of endogenous nitric oxide. Science. 2003; 299:896–899. [PubMed: 12574632]

45. Seale P, Kajimura S, Yang W, Chin S, Rohas LM, Uldry M, Tavernier G, Langin D, Spiegelman BM. Transcriptional control of brown fat determination by PRDM16. Cell Metab. 2007; 6:38–54. [PubMed: 17618855]

46. Siervo M, Jackson SJ, Bluck LJC. In-vivo nitric oxide synthesis is reduced in obese patients with metabolic syndrome: application of a novel stable isotopic method. J Hypertens. 2011; 29:1515–1527. [PubMed: 21720276]

47. Liese AD, Nichols M, Sun XZ, D' Agostino RB, Haffner SM. Adherence to the DASH Diet Is Inversely Associated With Incidence of Type 2 Diabetes: The Insulin Resistance Atherosclerosis Study. Diabetes Care. 2009; 32:1434–1436. [PubMed: 19487638]

48. Carter P, Gray LJ, Troughton J, Khunti K, Davies MJ. Fruit and vegetable intake and incidence of type 2 diabetes mellitus: systematic review and meta-analysis. BMJ. 2010; 341:c4229. [PubMed: 20724400]
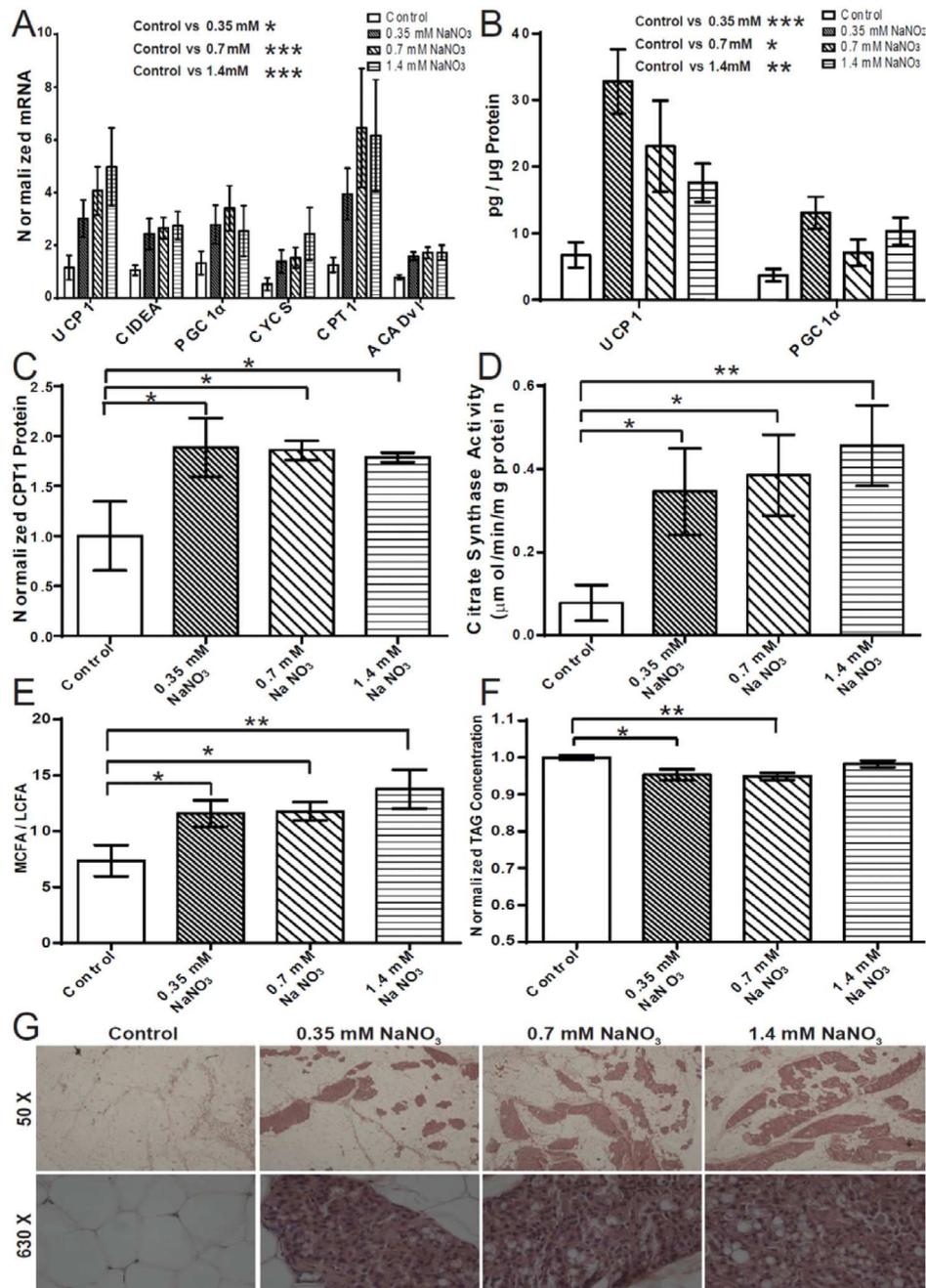
Fig. 1.
Dietary nitrate induces a brown adipocyte-like phenotype in white adipose tissue (WAT) *in vivo*. (*A*) Increased expression of brown-adipocyte specific genes in subcutaneous WAT of nitrate treated rats (Two-way ANOVA, Control vs. 0.35 mM $NaNO_3$ P 0.01, Control vs. 0.7 mM $NaNO_3$ P 0.001, Control vs. 1.4 mM P 0.0001). (*B*) Increased concentration of brown-adipocyte specific proteins in subcutaneous WAT of nitrate treated rats determined by ELISA (Two-way ANOVA, Control vs. 0.35 mM $NaNO_3$ P 0.001, Control vs. 0.7 mM $NaNO_3$ P 0.05, Control vs. 1.4 mM P 0.01) (*C*) Increased concentration of carnitine

palmitoyltransferase 1 (CPT1) protein in subcutaneous WAT of nitrate treated rats determined by immunoblotting (One-way ANOVA, Control vs. 0.35 mM NaNO$_3$ P 0.05, Control vs. 0.7 mM NaNO$_3$ P 0.05, Control vs. 1.4 mM NaNO $_3$ P 0.05). (*D*) Increased citrate synthase activity in subcutaneous WAT of nitrate treated rats (One-way ANOVA, Control vs. 0.35 mM NaNO$_3$ P 0.05, Control vs. 0.7 mM NaNO $_3$ P 0.05, Control vs. 1.4 mM P 0.01) (*E*) The medium chain fatty acid (MCFA) / long chain fatty acid (LCFA) ratio in WAT from nitrate treated rats (One-way ANOVA, Control vs. 0.35 mM NaNO$_3$ P 0.05, Control vs. 0.7 mM NaNO$_3$ P 0.05, Control vs. 1.4 mM NaNO $_3$ P 0.01). (*F*) LC-MS analysis of total triacylglycerols (TAGs) from WAT indicates decreased total TAGs stored in the WAT of nitrate treated rats (One-way ANOVA, Control vs. 0.35 mM NaNO$_3$ P 0.01, Control vs. 0.7 mM NaNO$_3$ P 0.01). (*G*) Haematoxylin and eosin staining of inguinal WAT of control and nitrate treated rats. Cumulative data from a total of 6 independent observations are shown. Data are represented as Mean ± SEM. * P 0.05, ** P 0.01, *** P 0.001, **** P 0.0001.
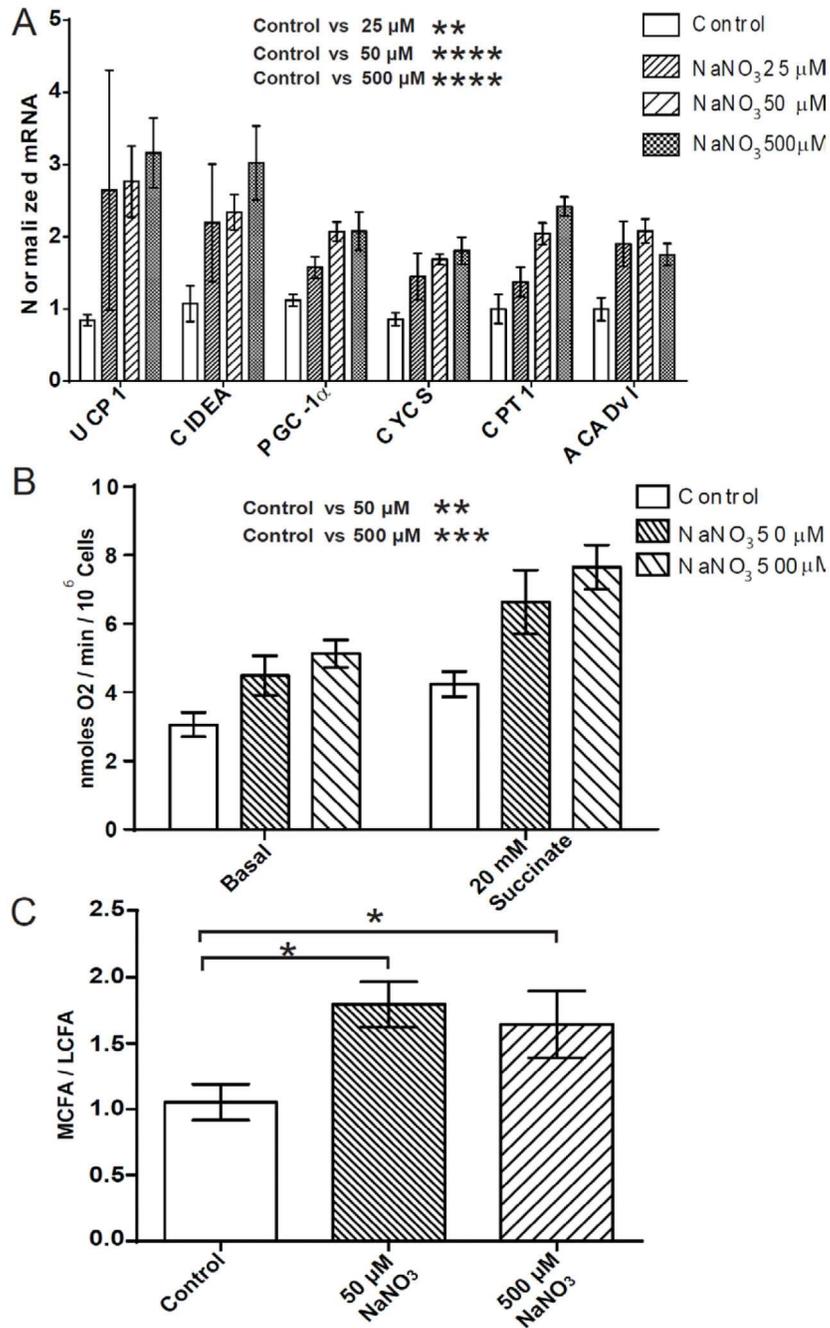
Fig. 2.
Nitrate stimulates expression of brown adipocyte-specific genes and induces an oxidative phenotype in primary white adipocytes. (*A*) The expression of brown adipocyte-specific genes in primary white adipocytes treated with nitrate (25 μM $NaNO_3$, 50 μM $NaNO_3$ and 500 μM $NaNO_3$) (Two-way ANOVA, Control vs. 25 μM $NaNO_3$ P 0.01, Control vs. 50 μM $NaNO_3$ P 0.0001, Control vs. 500 μM $NaNO_3$ P 0.0001). (*B*) Basal and stimulated (succinate 20 mM) oxygen consumption was increased in white adipocytes treated with nitrate, normalized to 10^6 cells (Two-way ANOVA, Control vs. 50 μM $NaNO_3$ P 0.01,

Control vs. 500 μM NaNO$_3$ P 0.001). (*C*) The medium chain fatty acid (MCFA) / long chain fatty acid (LCFA) ratio was increased in white adipocytes with nitrate treatment (ANOVA, Control vs. 50 μM NaNO$_3$ P 0.05, Control vs. 500 μM NaNO $_3$ P 0.05). Cumulative data from a total of 4 independent observations are shown. Data are represented as Mean ± SEM. * P 0.05, ** P 0.01, *** P 0.001, **** P < 0.0001.
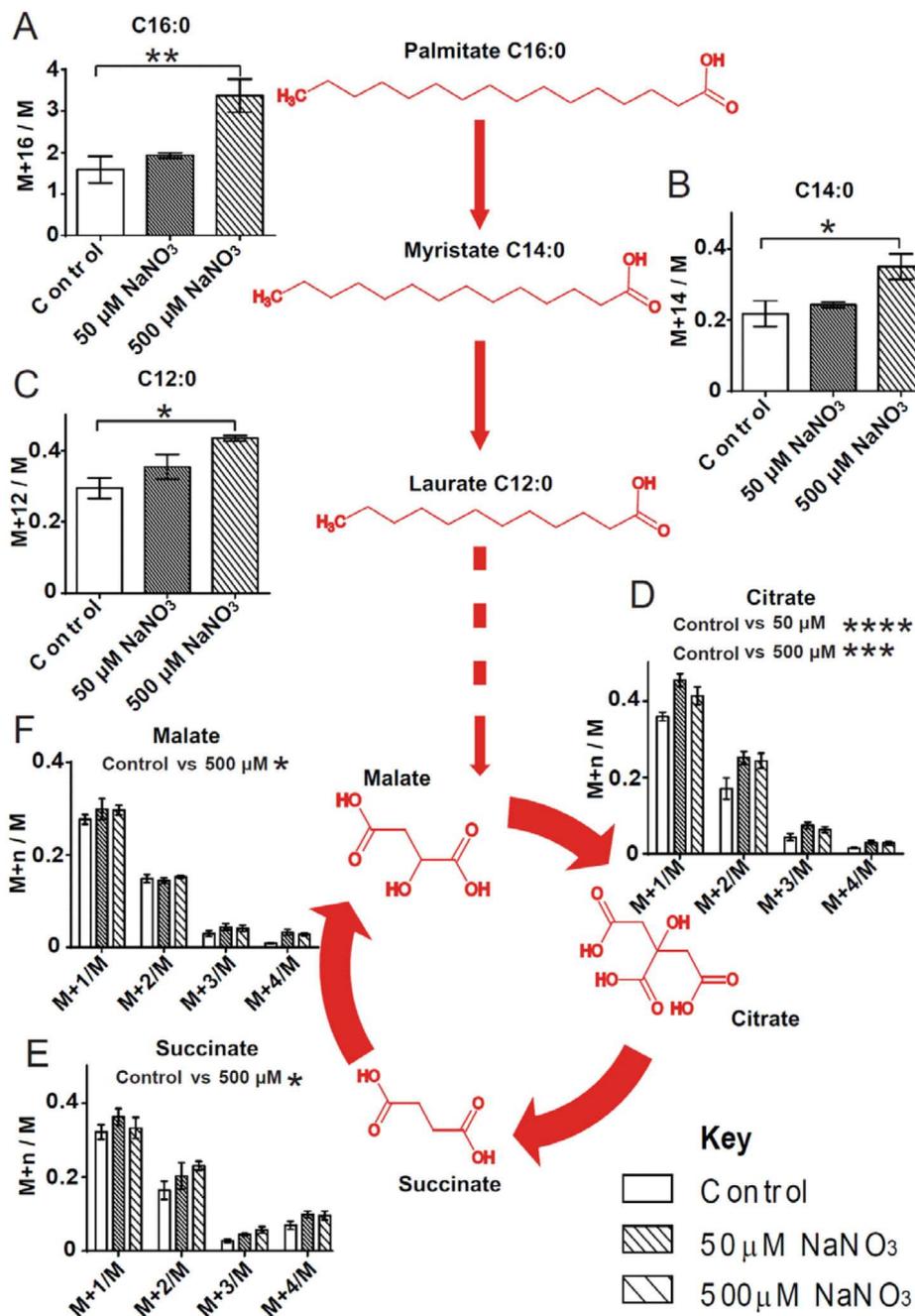
Fig. 3.

Fatty acid uptake and β-oxidation is increased in nitrate treated primary white adipocytes characteristic of the browning response. (*A*) ^{13}C-enrichment of palmitate (C16:0) was significantly increased in nitrate treated adipocytes (One-way ANOVA, P 0.01). (*B*) ^{13}C-enrichment of myristate (C14:0) was significantly increased in nitrate treated adipocytes (One-way ANOVA, P 0.05). (*C*) ^{13}C-enrichment of laurate (C12:0) was significantly increased in nitrate treated adipocytes (One-way ANOVA, P 0.05). (*D*) ^{13}C-enrichment of citrate was significantly increased in nitrate treated adipocytes (Two-way ANOVA, P

0.0001, Control vs. 50 μM NaNO$_3$ P   0.0001, Control vs. 500 μM NaNO $_3$ P   0.001) (*E*) ^{13}C-enrichment of succinate was significantly increased in nitrate treated adipocytes (Two-way ANOVA, P   0.05, Control vs. 500 μM NaNO $_3$ 0.05). (*F*) ^{13}C-enrichment of malate was significantly increased in nitrate treated adipocytes (Two-way ANOVA, P 0.05, Control vs. 500 μM NaNO$_3$ P   0.05). Red highlighting indicates increased enrichment. Cumulative data from a total of 4 independent observations are shown. Data are represented as Mean ± SEM. * P   0.05, ** P   0.01,*** P   0.001, **** P < 0.0001.
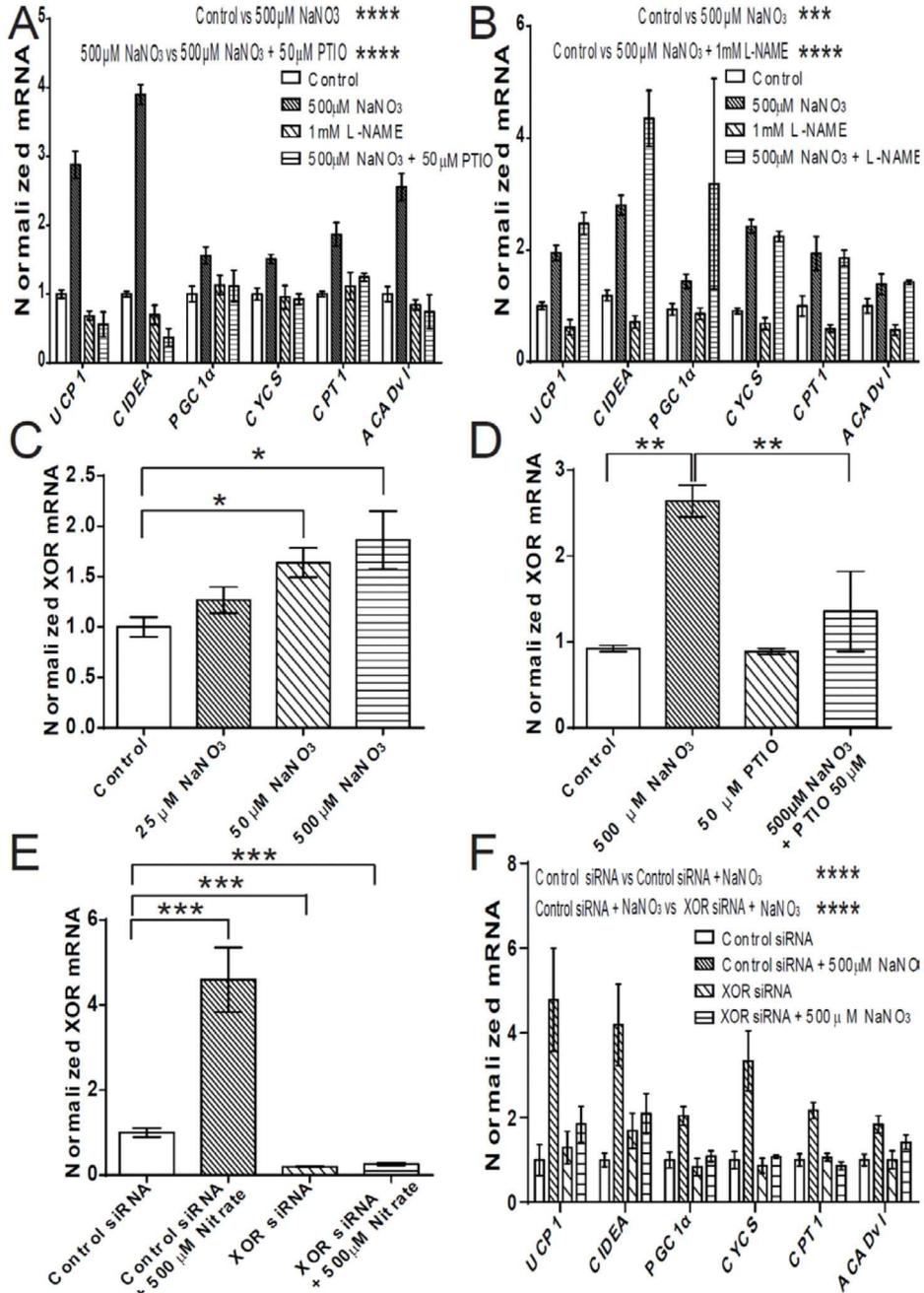
Fig. 4.
Nitrate functions through the nitrate-nitrite-NO pathway to induce browning of white adipocytes. (*A*) Brown adipocyte-specific gene expression in primary adipocytes treated with the NO scavenger PTIO (50 μM) with and without 500 μM NaNO$_3$ (Two-way ANOVA, Control vs. 500 μM NaNO$_3$ P 0.0001, 500 μM NaNO$_3$ vs. 500 μM NaNO$_3$ + 50 μM PTIO P 0.0001) (n = 3). (*B*) Brown adipocyte-specific gene expression in primary adipocytes treated with the NOS inhibitor L-NAME (1 mM) with and without 500 μM NaNO$_3$ (Two-way ANOVA, Control vs. 500 μM NaNO$_3$ P 0.001, Control vs. 500 μM

NaNO$_3$ + 1 mM L-NAME P 0.0001) (n = 3). (*C*) The expression of xanthine oxidoreductase (XOR) in primary white adipocytes treated with nitrate (25 μM, 50 μM, 500 μM) (One-way ANOVA, Control vs. 50 μM NaNO$_3$ P 0.05, Control vs. 500 μM NaNO$_3$ P 0.05) (n = 4). (*D*) XOR expression in primary adipocytes treated with the NO scavenger PTIO (50 μM) with and without 500 μM NaNO$_3$ (One-way ANOVA, Control vs. 500 μM NaNO$_3$ P 0.01, 500 μM NaNO$_3$ vs. 500 μM NaNO$_3$ + 50 μM PTIO P 0.01) (n = 3). (*E*) XOR expression in primary adipocytes treated with negative control siRNA or siRNA against XOR with and without 500 μM NaNO$_3$ (n = 3 / group) (One-way ANOVA, Control siRNA vs.Control siRNA + 500 μM NaNO$_3$ P 0.001, Control siRNA vs XOR siRNA P 0.001, Control siRNA vs XOR siRNA+ 500 μM NaNO$_3$ P 0.001) (*F*) Brown adipocyte-specific gene expression in primary adipocytes treated with negative control siRNA or siRNA against XOR with and without 500 μM NaNO$_3$ (n = 3 / group) (Two-way ANOVA, Control siRNA vs Control siRNA + 500 μM NaNO$_3$ P 0.0001, Control siRNA + 500 μM NaNO$_3$ vs XOR siRNA+ 500 μM NaNO$_3$ P 0.0001, XOR siRNA vs XOR siRNA+ 500 μM NaNO$_3$ not significant). Data are represented as Mean ± SEM. * P 0.05, ** P 0.01, *** P 0.001, **** P < 0.0001.
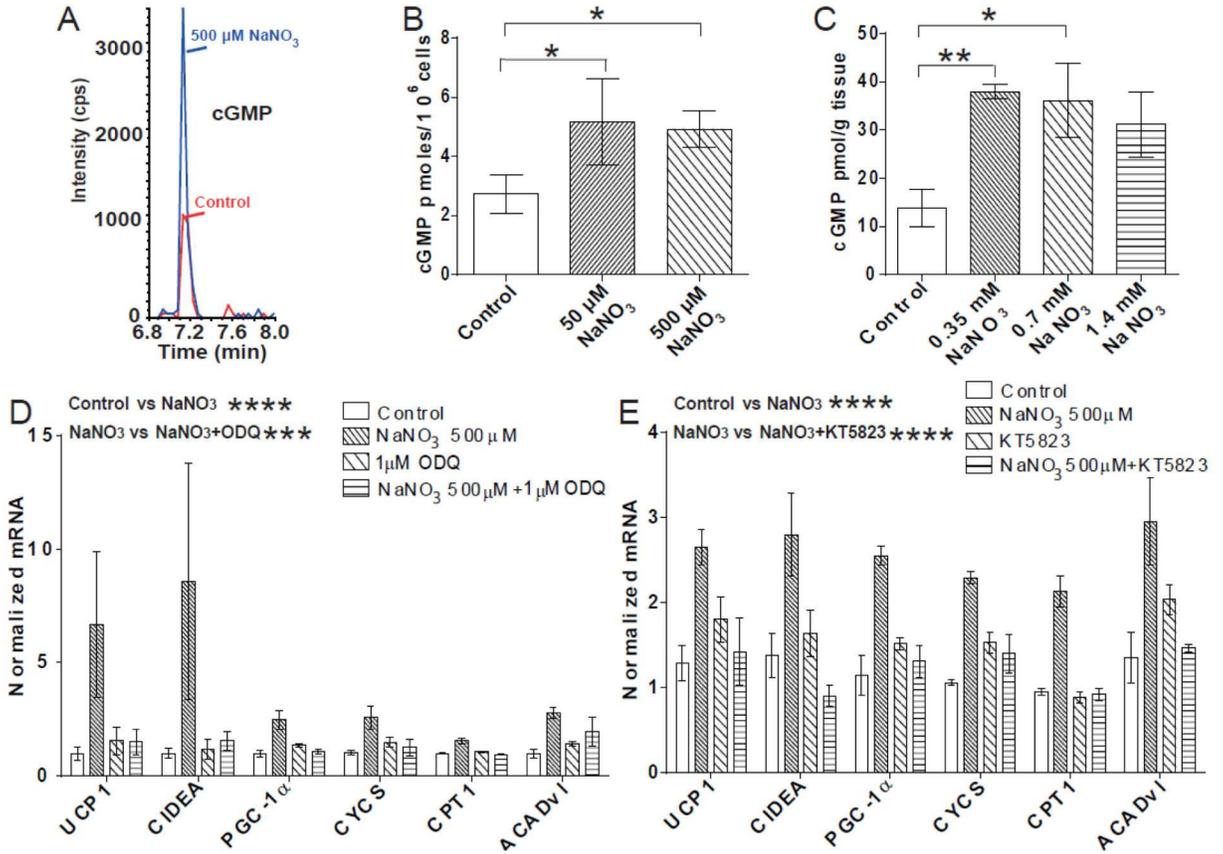
Fig. 5.

cGMP signaling mediates the nitrate stimulated browning response in white adipocytes. (*A*) LC-MS chromatograms of typical peaks for cGMP from control and 500 μM NaNO$_3$ treated primary adipocytes. (*B*) The concentration of cGMP increases in primary white adipocytes treated with nitrate (ANOVA, P 0.05, Control vs. 50 μM NaNO$_3$ P 0.05, Control vs. 500 μM NaNO$_3$ P 0.05) (n = 4). (*C*) The concentration of cGMP increases in white adipose tissue of rats treated with nitrate (0.35 mM NaNO$_3$, 0.7 mM NaNO$_3$ and 1.4 mM NaNO$_3$) (ANOVA, P < 0.05, Control vs. 0.35 mM NaNO$_3$ P 0.01, Control vs. 0.7 mM NaNO$_3$ P 0.05, Control vs. 1.4 mM NaNO$_3$, P = 0.07) (n = 6). (*D*) Primary adipocytes treated with the guanylyl cyclase inhibitor ODQ (1 μM) with and without 500 μM NaNO$_3$ (Two-way ANOVA, Control vs. 500 μM NaNO$_3$ P 0.0001, 500 μM NaNO$_3$ vs. 500 μM NaNO$_3$ + 1 μM ODQ P 0.001) (n = 6). (*E*) Primary adipocytes treated with the protein kinase G inhibitor KT5823 (1 μM) with and without 500 μM NaNO$_3$ (Two-way ANOVA, Control vs. 500 μM NaNO$_3$ P 0.0001, 500 μM NaNO$_3$ vs. 500 μM NaNO$_3$ + 1 μM KT5823 P 0.0001) (n = 3). Data are represented as Mean ± SEM. * P 0.05, ** P 0.01, **** P < 0.0001.
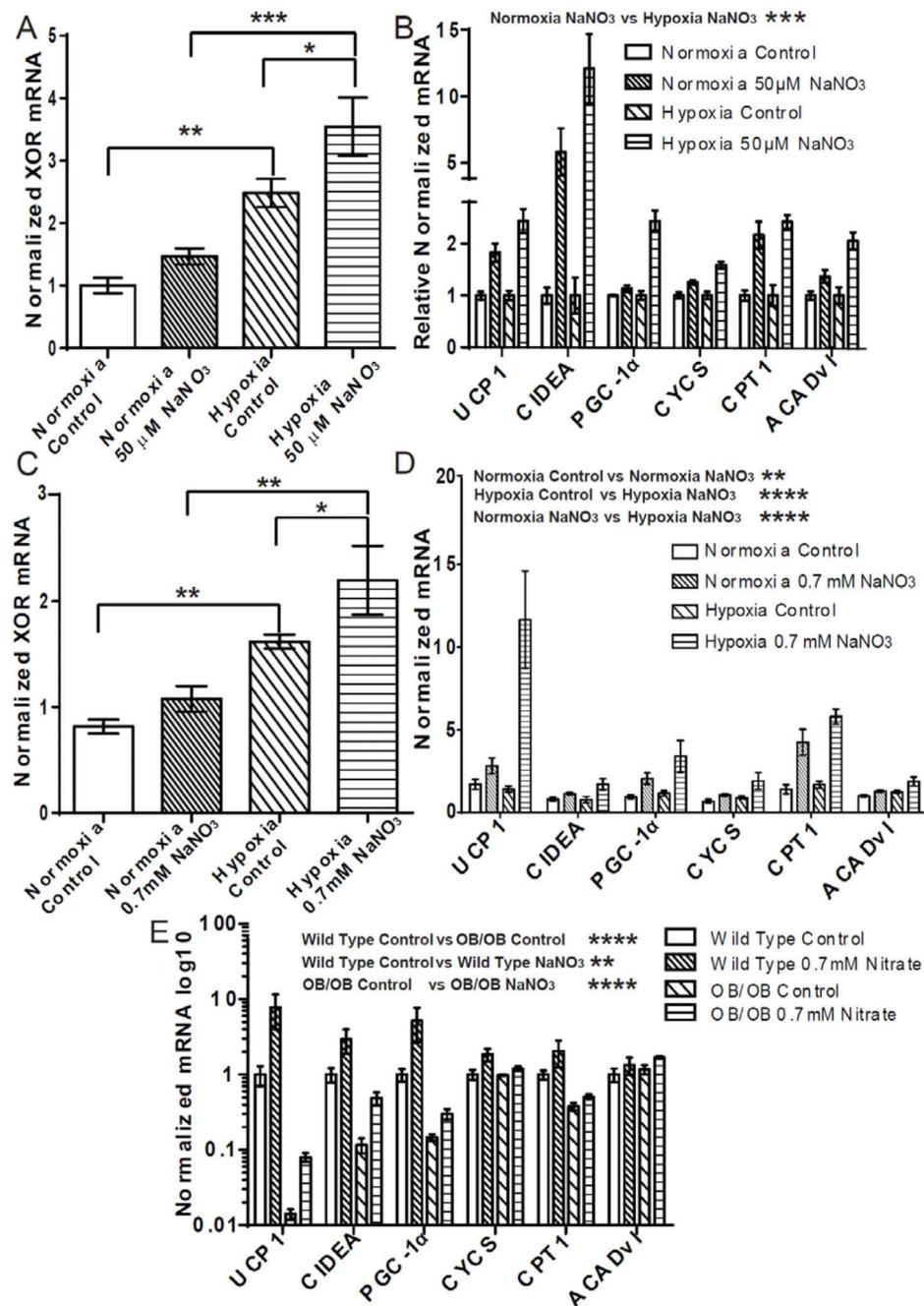
Fig. 6.
The nitrate stimulated browning response is enhanced in hypoxia. (*A*) Nitrate (50 μM NaNO₃) induced expression of xanthine oxidoreductase (XOR) in white adipocytes is increased in hypoxia (Two-way ANOVA, Normoxia Control vs. Hypoxia Control P 0.01, Normoxia NaNO₃ vs. Hypoxia NaNO₃ P 0.001, Hypoxia Control vs. Hypoxia NaNO ₃ P 0.05) (n = 4). (*B*) The expression of brown adipocyte-specific genes in primary white adipocytes treated with nitrate (50 μM NaNO₃) in normoxia or hypoxia and normalized to relevant control (normoxia 50 μM nitrate normalized to normoxia control, hypoxia 50 μM

nitrate normalized to hypoxia control) (Two-way ANOVA, Normoxia NaNO$_3$ vs. Hypoxia NaNO$_3$ P   0.001) (n = 4). (*C*) The expression of XOR in white adipose tissue (WAT) of nitrate treated (0.7 mM NaNO$_3$) rats is increased in hypoxia (Two-way ANOVA, Normoxia Control vs. Hypoxia Control P   0.01, Normoxia NaNO $_3$ vs. Hypoxia NaNO$_3$ P   0.01, Hypoxia Control vs. Hypoxia NaNO$_3$ P   0.05) (n = 5). (*D*) The increased expression of brown-adipocyte specific genes in WAT of nitrate treated rats is enhanced during hypoxia (Two-way ANOVA, Normoxia 0.7 mM NaNO$_3$ vs. Hypoxia 0.7mM NaNO$_3$, P < 0.0001) (n = 5). (*E*) The reduced expression of brown adipocyte-specific genes in WAT of the *ob/ob* mouse compared to wild type controls is partially restored following nitrate treatment. (Two-way ANOVA, Wild Type Control vs. *ob/ob* Control P   0.0001, Wild Type Control vs. Wild Type NaNO$_3$ P   0.01, *ob/ob* Control vs. *ob/ob* NaNO$_3$ P   0.0001) Data are represented as Mean ± SEM. * P   0.05, ** P   0.01, *** P   0.001, **** P < 0.0001.
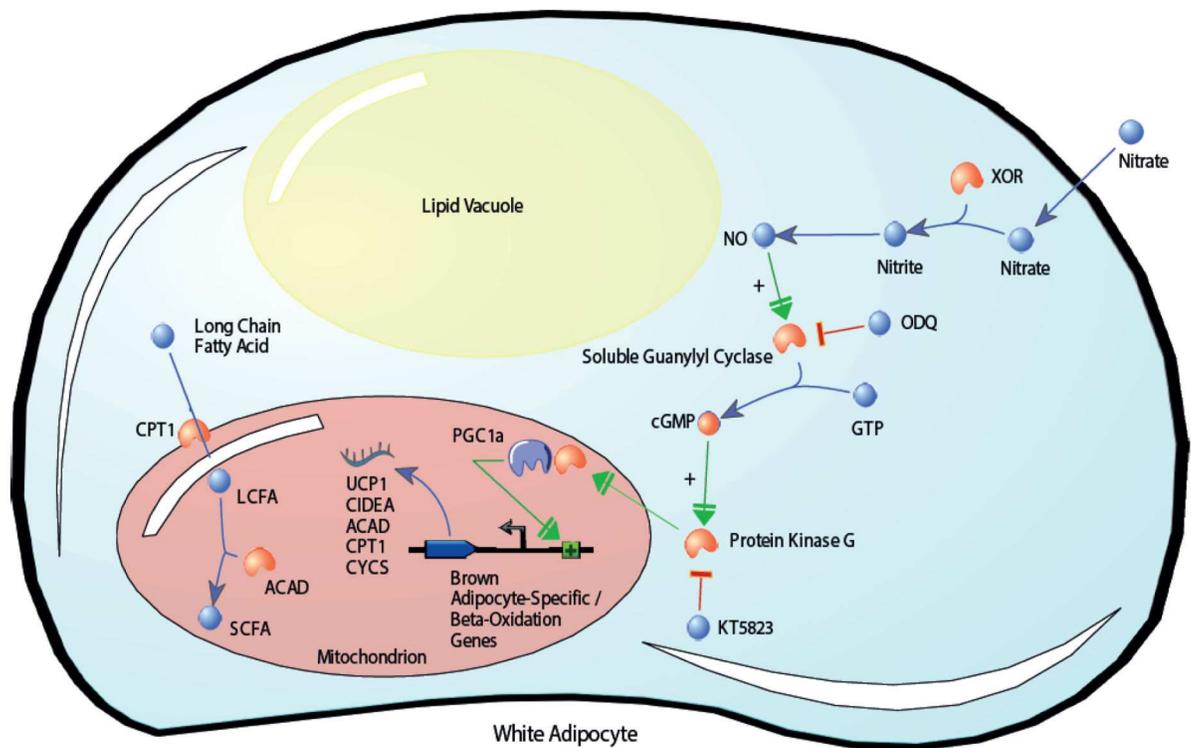
Fig. 7.
Proposed mechanism for nitrate-induced browning of white adipocytes. After entering the cell, nitrate is reduced first to nitrite, then to nitric oxide (NO). NO increases cGMP production via soluble guanylyl cyclase activation. Increased cGMP concentrations activate PKG, increasing the expression of PGC-1α and key browning genes. Increased expression of brown adipocyte-specific and β-oxidation pathway genes confers an oxidative brown adipocyte-like functional phenotype on the white adipocytes. ACAD, acyl-CoA dehydrogenase; CIDEA, cell death-inducing DFFA-like effector a; cGMP, cyclic guanosine monophosphate; CPT1, carnitine palmitoyltransferase; CYCS, cytochrome c; GTP, Guanosine triphosphate; LCFA, long chain fatty acid; NO, nitric oxide; ODQ, 1H-[1,2, 4]oxadiazolo[4,3-a]quinoxalin-1-one; PGC1α, peroxisome proliferator-activated receptor gamma coactivator 1-alpha; SCFA, short chain fatty acid; UCP1, uncoupling protein 1; XOR, xanthine oxidoreductase.